Chapter 15: Maps of Exogenic Structures

THE SURFACE of the Earth is shaped by a wide range of exogenic processes. Exogenic structures originate from processes at or near the surface of the Earth. In contrast, endogenic deformation structures are created by mechanisms originating from within the Earth. The structures discussed in preceeding chapters are all formed by endogenic processes (e.g., folds, faults, igneous intrusions and extrusions). Four main types of exogenic structures are considered here: impact structures, landslides, sinkholes, and glacial structures. Knowledge of these distinct features is essential for interpreting geological maps correctly.

Contents: Impact structures are illustrated in section 15-1. Examples of landslides are discussed in section 15-2. Sinkholes and glacial patterns constitute sections 15-3 and 15-4, respectively.

15-1 Impact structures

The solar system formed about five billion years ago by gravitational accretion of matter from a solar nebula. The protoplanets formed in molten state, because the reduction of potential energy by the gravitational collapse of the solar matter released heat. The surfaces of the terrestrial planets had sufficiently cooled to solidify about four billion years ago. The surfaces of the Moon, and of Mars and Mercury are only minimally affected by erosion processes and display a large number of pristine *impact structures* or *astroblemes*, that have battered their crusts since their early formation. Counting and dating of the lunar and Martian craters have revealed that the planets of the solar system suffered particularly frequent impacts about four billion years ago, when the majority of the craters were formed.

Size-frequency distribution counts further suggest that the Earth, also, must have hosted an enormous number of impact structures. Estimates for the past two billion years include twenty craters larger than one hundred kilometers in diameter, 6,000 craters of five to one hundred kilometers in diameter, and 100,000 craters of one to five kilometers in diameter. However, the

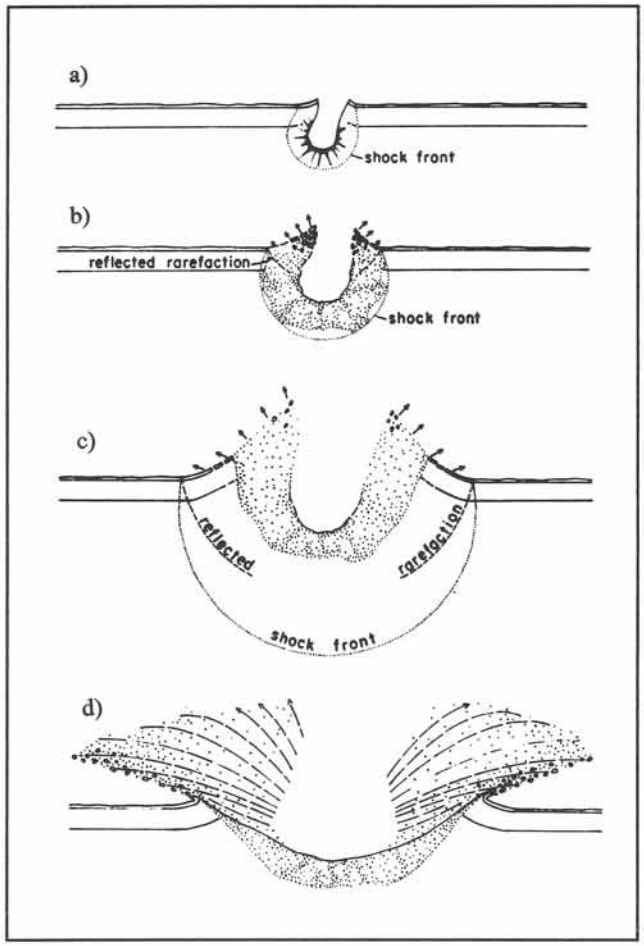

Figure 15-1: *a) to d) Schematic cross-sections of a developing impact crater. a) Propagating shock front and expanding impact cavity. b) Shock front envelopes partly fused and brecciated rock. c) Material behind rarefaction limit, including meteoritic fragments, is ejected. d) Margins of the crater are backfolded, leaving debris inside and outside the crater wall.*

average continental erosion rate of about one hundred meters per million years rapidly excavates and removes most of these impact structures. Consequently, we can expect to find only the remnants of relatively young impact structures or the scars of older impacts so big that they extended well below the reach of subsequent erosion depths. So far, only about two hundred impact craters have been convincingly identified on Earth; most of them are located in tectonically stable Precambrian terrains.

The formation of an *impact crater* is illustrated in Figure 15-1a to d. Rock, compressed by the initial impact, partly fractures and melts, but it, also, rebounds elastically to eject debris fragments and to backfold any sedimentary layers in the crater rim. The final crater morphology comprises an elevated rim, radial ejecta and fracture patterns, and a central depression - sometimes hosting a central mound and circumferential or annular graben (Fig. 15-2a & b). The central mound occurs only in craters larger than about five kilometers and results from the tendency for the center to take up most of the elastic recovery, leaving an annular depression between the central mound and the crater rim (Fig. 15-2).

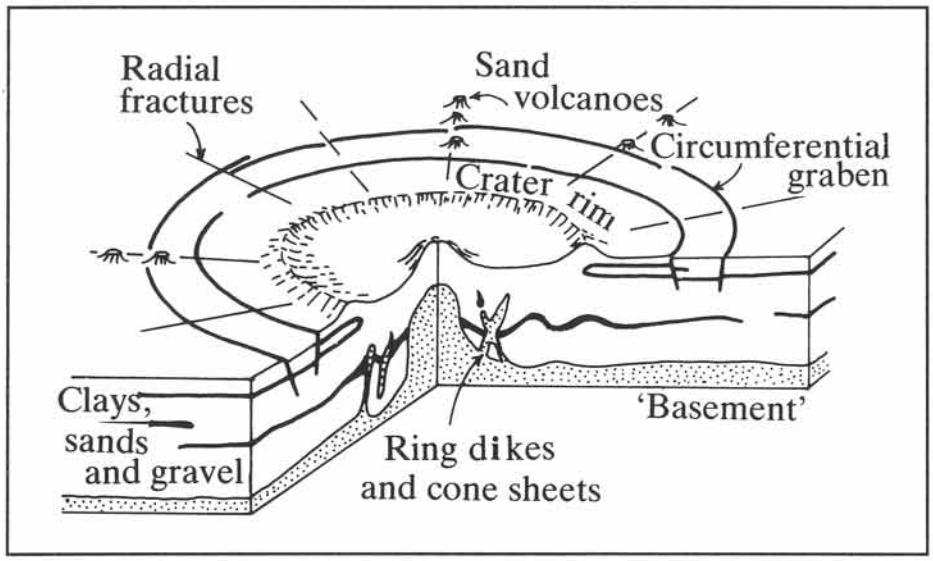

Figure 15-2: *Structural elements of an impact crater.*

Systematic studies of impact structures received

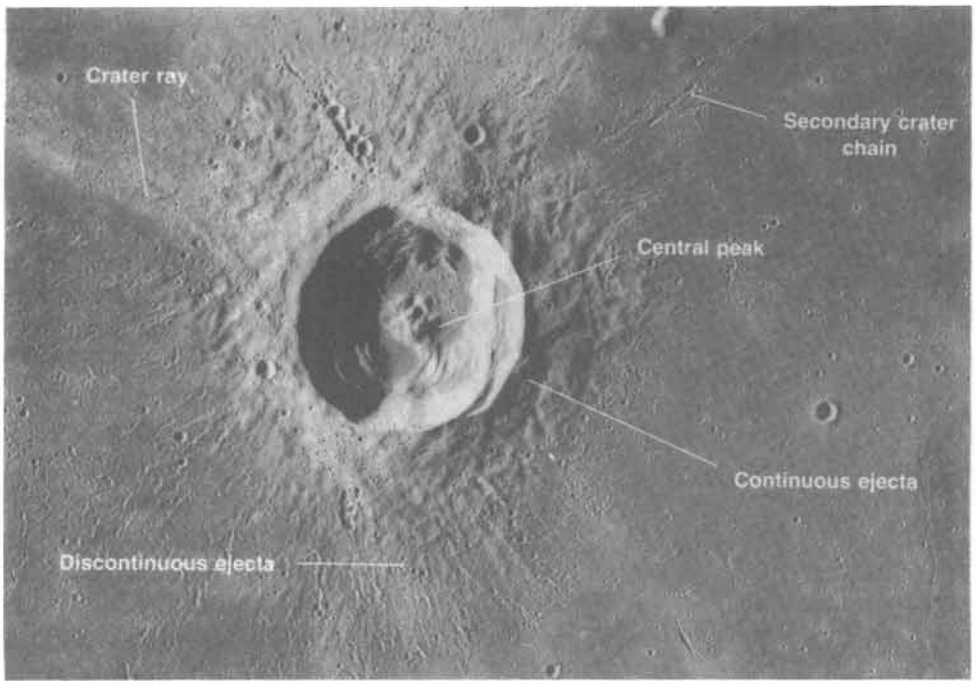

Figure 15-3a: *Crater Euler and central peaks measure twenty kilometers across, Mare Imbrium, Moon.*

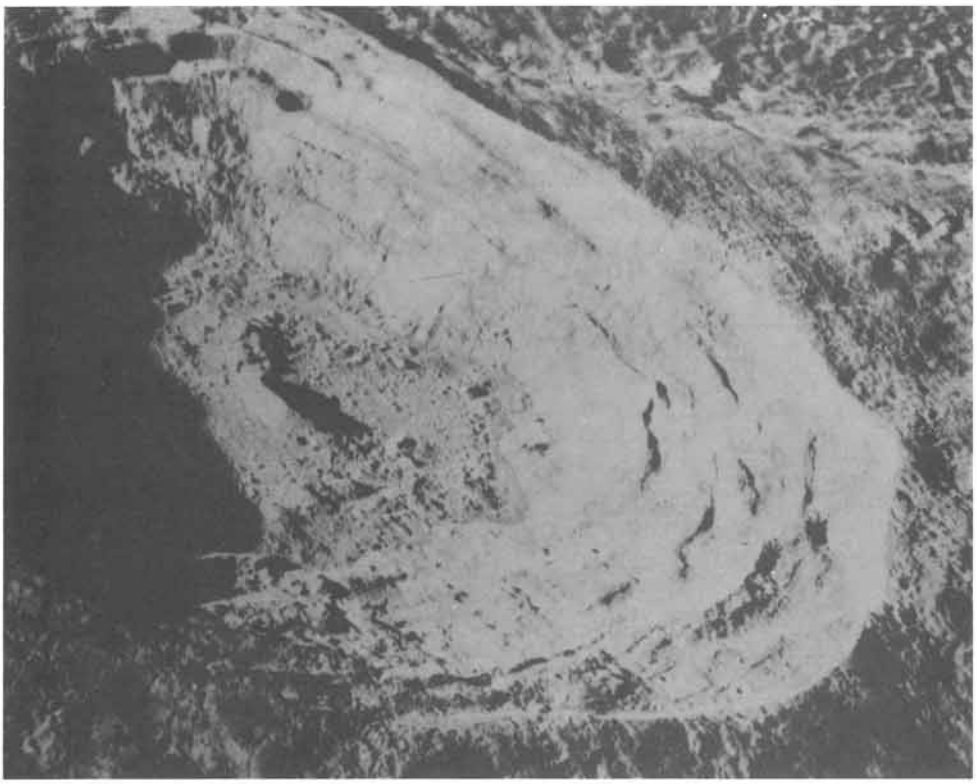

Figure 15-3b: *Crater Aristarchus, measuring forty kilometers across, with internal slump terraces, Moon.*

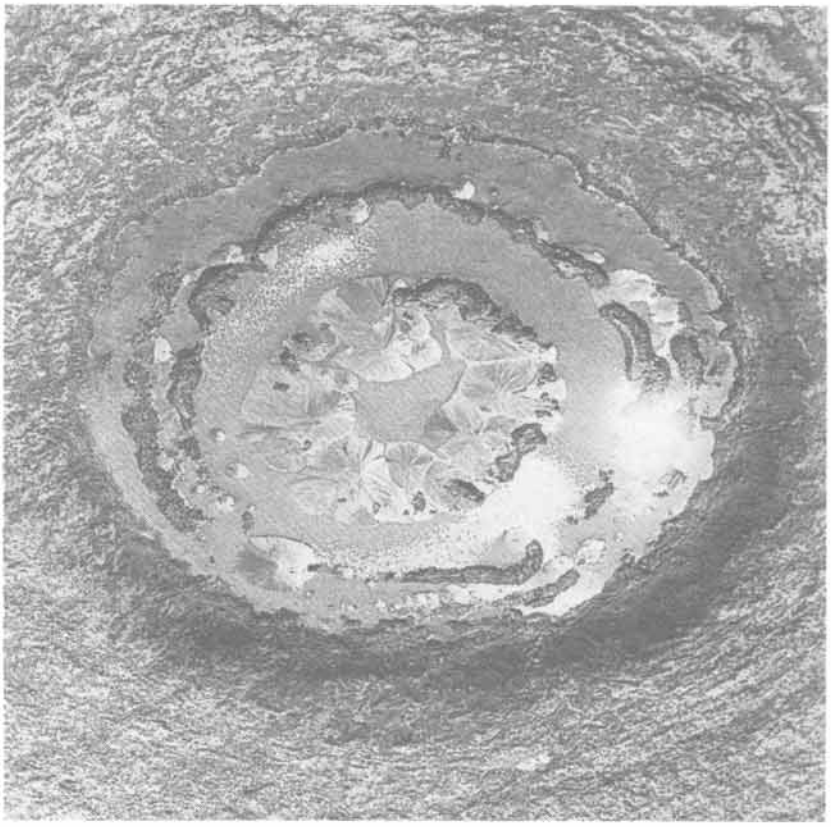

Figure 15-4: *Crater caused by ground blast test. Internal slump terraces are partially submerged by ground water.*

a major boost after detailed images of lunar craters were acquired by Apollo flights of the late 1960's and early 1970's (Figs. 15-3a & b). These images provided clear examples of large impact craters with central mounds and internal slump terraces. Such slump terraces have been reproduced in experimental ground blasts, using dynamite to simulate the effect of a meteoritic impact (Fig. 15-4). The elevated crater rim is a rather characteristic feature of impact craters.

Theoretical studies show that only larger *meteorites*, with masses in excess of ten tons, have enough kinetic energy to break through the Earth's atmosphere without being slowed down. Their impact speeds are about ten to fifty kilometers per second. Bodies smaller than one ton completely disintegrate upon entry into the atmosphere. Parts of bodies of intermediate size may reach the Earth's surface, but with their speed greatly reduced, approaching free-fall velocities of about one hundred meters per second. The well-known Meteor Crater, Arizona, 1.3 kilometers wide and two hundred meters deep (Fig. 15-5), is thought to

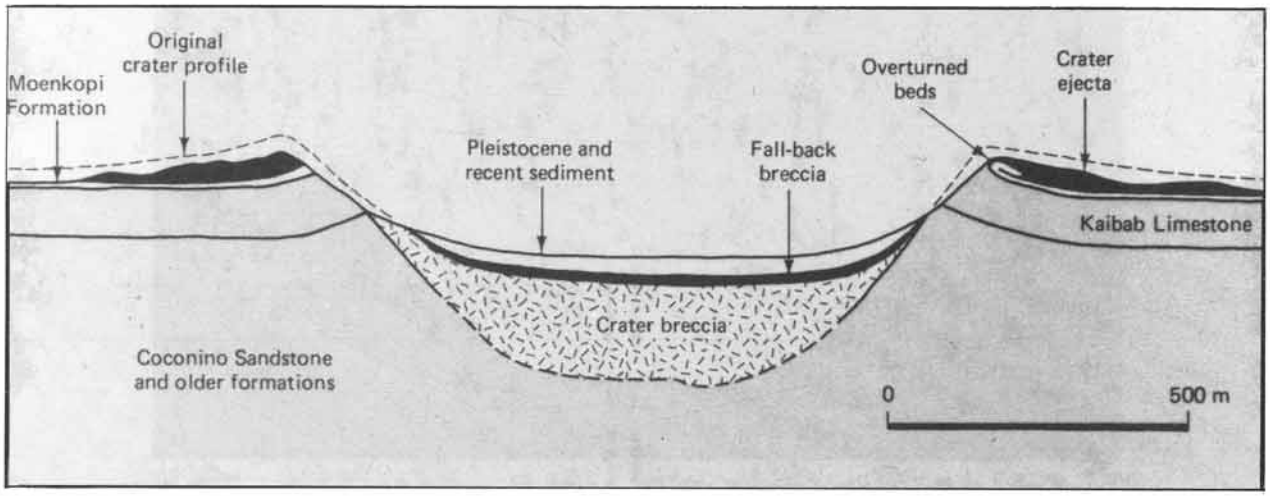

Figure 15-5: *Geologic cross-section of Meteor Crater, Arizona.*

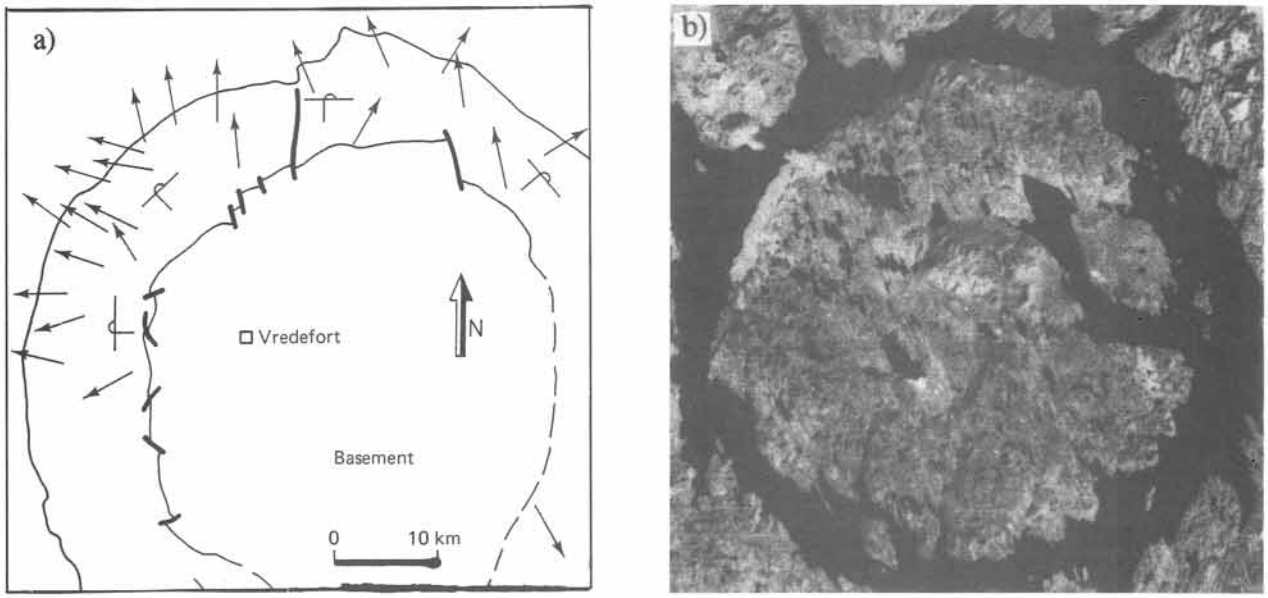

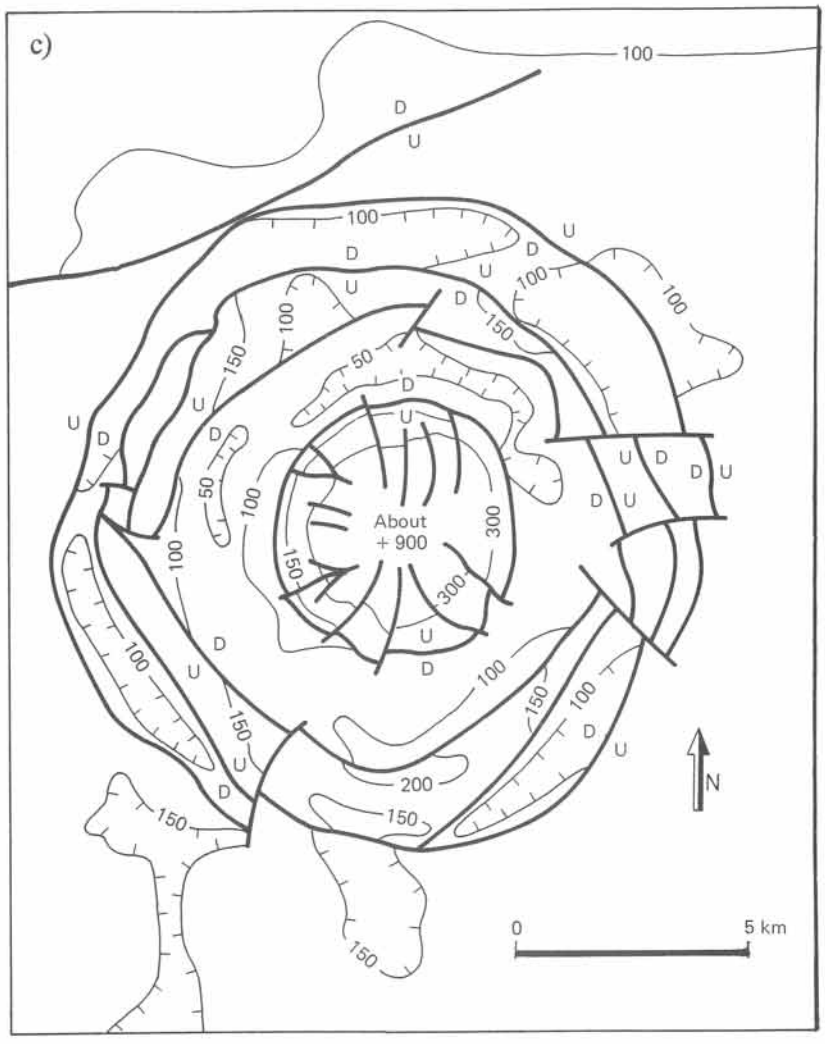

Figure 15-6: *Sketch maps and Landsat image of impact structures (astroblemes): (a) Vredefort, South Africa, (b) Manicouagan, Quebec, and (c) Wells Creek, Tennessee. Arrows in the overturned rimrock at Vredefort indicate shockwave propagation direction, inferred from shatter cones.*

have been formed by a meteorite of only 25 meters in diameter with an impact velocity of fifteen kilometers per second.

Many subcircular structures, now known to be of impact origin, were initially thought to be of igneous origin, because of the morphological similarities between impact craters and igneous craters. Additionally, impact melts may form rocks, resembling *pseudotachylites* and *rhyolites*. However, the backfolding of the crater rim, formation of certain high-pressure minerals,

impact breccias, and so-called *shatter cones* all are unique for impact craters. Some of the best investigated impact structures are: Meteor Crater, Arizona (1.2 km); Grosses Bluff, Australia (3 km); Wells Creek, Tennessee (10 km); Ries basin, Germany (20 km); Vredefort ring, South Africa (40 km); Siljan ring, Sweden (50 km), and the Manicouagan and Sudbury rings, Canada (66 and 100 km). A satellite image of the Manicouagan astrobleme, impressed on the Canadian shield of Quebec, visualizes the broad central uplift and a water-filled peripheral depression (Fig. 15-6b). The Vredefort ring and Wells Creek structure are illustrated in the maps of Figure 15-6a and c.

The Siljan ring structure, Precambrian shield of Sweden, is a meteoritic impact crater with an outer rim diameter of 50 kilometers (Fig. 15-7a).

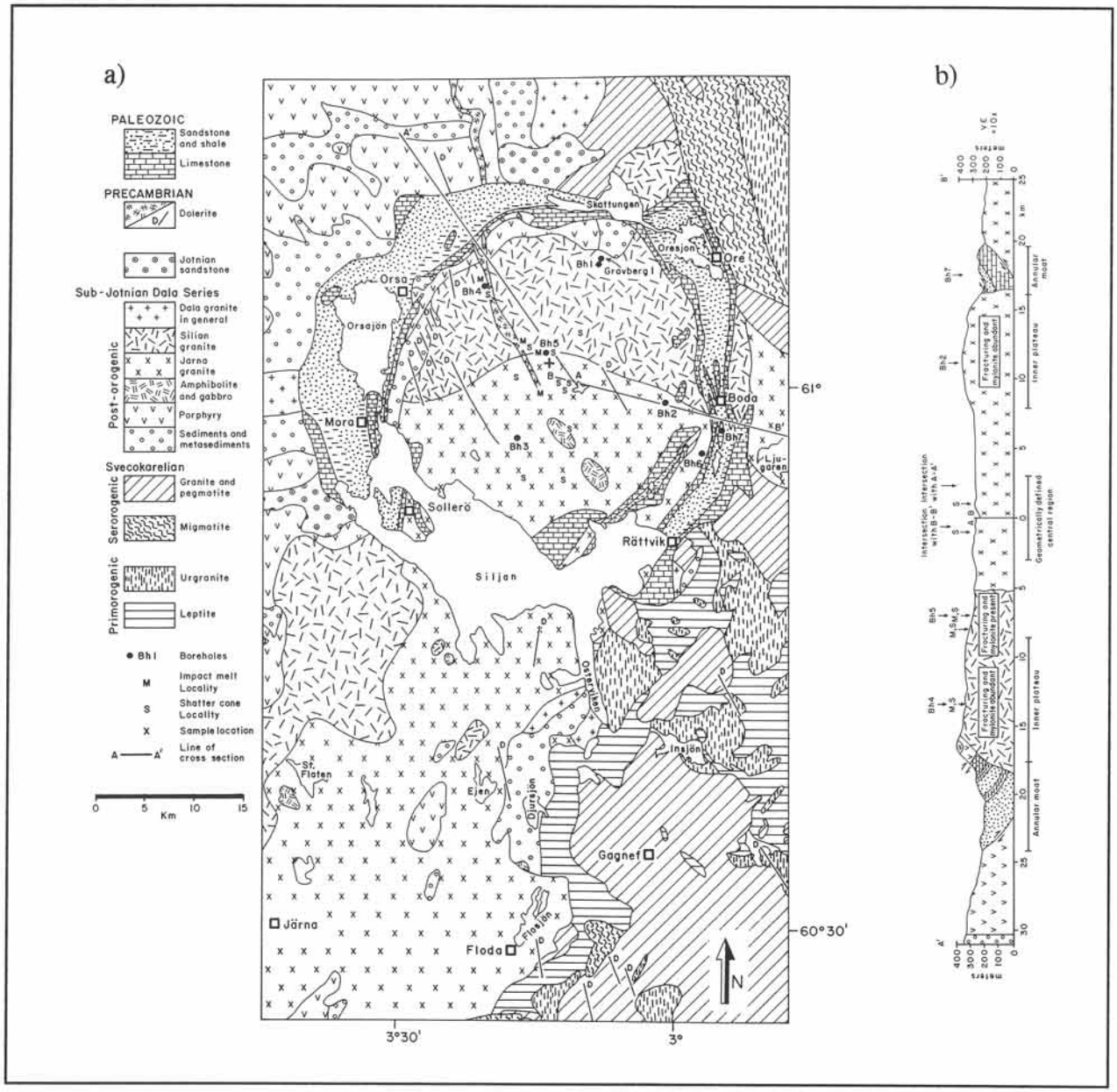

Figure 15-7: *a) & b) Geological map and cross-section of the Siljan impact ring, central Sweden. Indicated are the locations of seven shallow boreholes (Bh1-Bh7) and the first of two deep wells (Gravberg 1).*

Lower Paleozoic sedimentary rocks occupy an annular depression in the crater rim (Fig. 15-7b). The impact is of late Devonian age; it occurred about 360 million years ago. Two holes, up to seven kilometers deep, have been drilled into the floor of the Siljan crater. These expensive drillings explored for methane gas, that was speculated to have leaked from the mantle into fracture zones beneath the crater. Although huge quantities of methane are thought to occur dispersed in all planetary interiors, any fractures in the lower crust will heal and close by ductile creep. If any, significant gas concentrations in the Siljan area remain sealed in the mantle and were not encountered in any of the wells drilled.

☐Exercise 15-1: Research possible impact feature(s) relatively near to your home region, and summarize the main features and estimated age.

15-2 Landslides

Steeper slopes occupied by rock masses and soil may become unstable and collapse. The slope failure may involve movement of large volumes of rock, sometimes with devastating consequences if occurring in urban areas. A geological assessment, therefore, is important in the planning of new construction in order to investigate the stability of any slopes, supporting or surrounding the projected building site. An initial examination of existing survey maps may reveal whether any *landsliding* or *mass wasting* has been recognized in the area. The detached rock masses leave behind a distinct scar in the terrain with a typical spoon-shaped curvature (Fig. 15-8). The movement involves the formation of transverse normal faults across the slide mass with progressive loss of coherence, as the jumbled blocks move downward. The lower portion of the slump mass may consist of a *debris-flow*.

One of the grimmest examples of the seriousness of the threat posed by landsliding is illustrated by the 1970 rock avalanche of Yungay, Peru. A strong off-shore earthquake and the associated ground motion triggered the collapse of an already unstable north flank of the 6,700-meter-high Nevados Huascaran in the Peruvian Andes. A rock mass of millions of tons slid down the mountain side and fell for over one kilometer, disintegrating upon impact. It was accompanied by the melting of ice entrapped in the mass movement. The resulting debris-flow roared down the nearby valley floor, jumped a 200-meter-high ridge in the valley, and completely

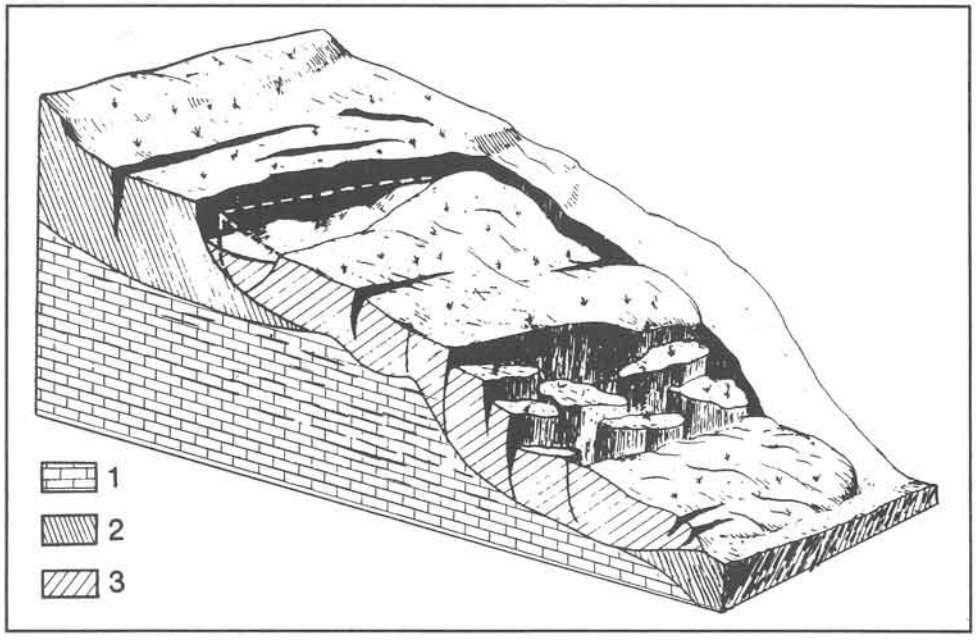

Figure 15-8: *Block diagram of idealized landslide. Legend shows: (1) solid bed rock, (2) poorly consolidated soil, (3) slump mass.*

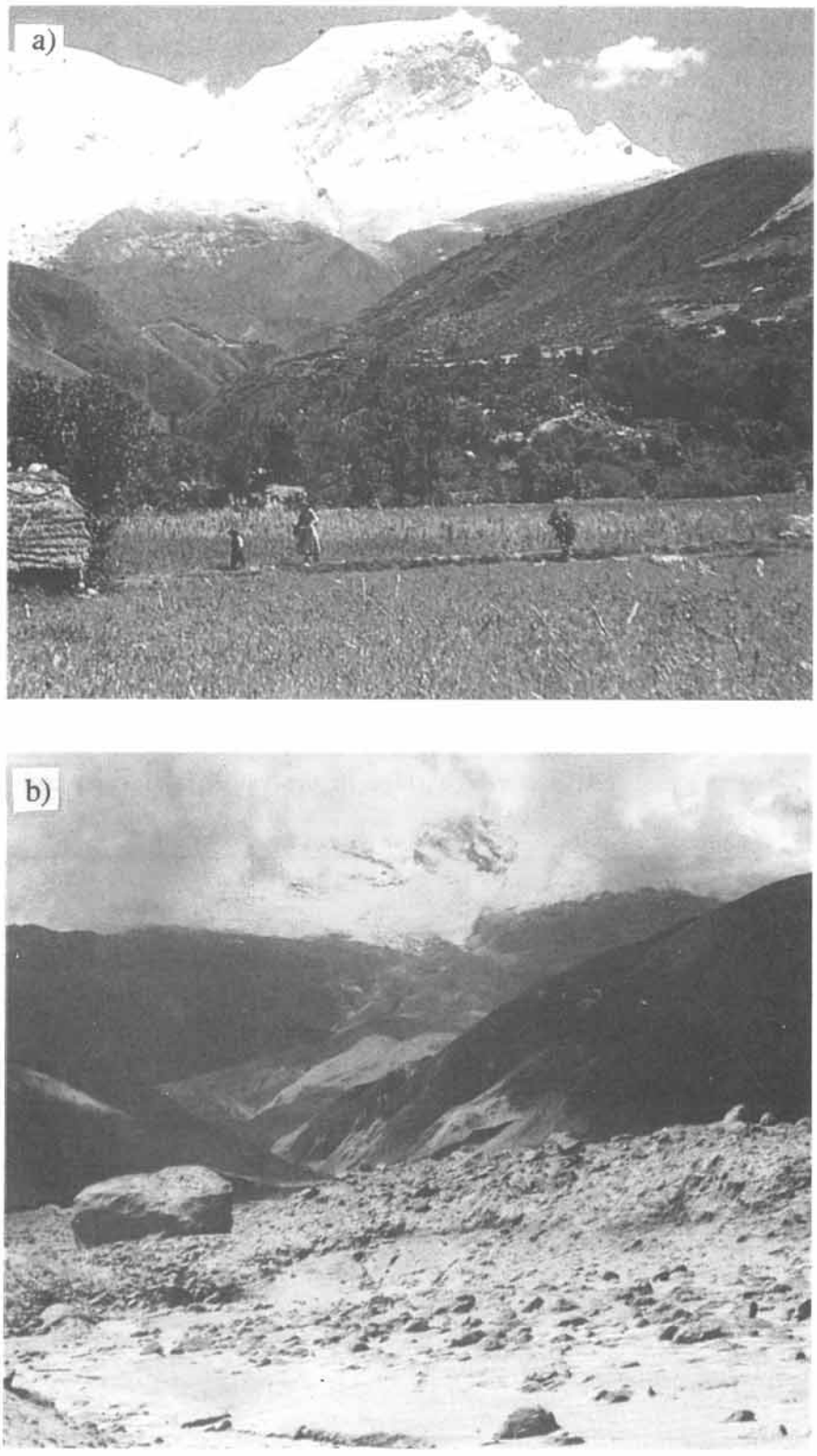

Figure 15-9: *a) & b) Views of the valley floor near Yungay: (a) before, and (b) after the arrival of a debris-flow from the Nevados Huascaran.*

buried the adjacent town of Yungay, fourteen kilometers away from the Huascaran (Fig. 15-9a & b). Ranrahirca, another town close to Yungay, was, also, erased by the mass movement, causing a total death toll of 20,000 people. The whole tragedy was completed in a few minutes. Rock avalanches may reach speeds of 200 kilometers per hour. Part of the rock movement is facilitated by compressed air, trapped underneath the slide mass.

Figure 15-10 illustrates a four-kilometer-long debris-flow, covering the snout of the Sherman Glacier, Alaska, that was triggered by the 1964 earthquake of magnitude 8.5. The same earthquake set up a tsunami, which swept the coast of the Gulf of Alaska. An entire ocean front district of Anchorage, Turnagain Heights, collapsed by landsliding over a clay bed, liquefied by the water pressure (Fig. 15-11). The event caused 131 deaths. Sliding was extensive, also, at the town of Valdez, where 31 persons were killed when an entire dock slid into the ocean. In an unprecedented move, Valdez was abandoned and rebuilt on more stable ground, seven kilometers away from its 1964 location. Landsliding need not necessarily be triggered by seismic ground movement. Figure 15-12 illustrates the erosion of the coastline by landsliding at

Figure 15-10: A huge rock avalanche (dark) covers the snout of the Sherman Glacier, Alaska. It was triggered by the 1964 earthquake.

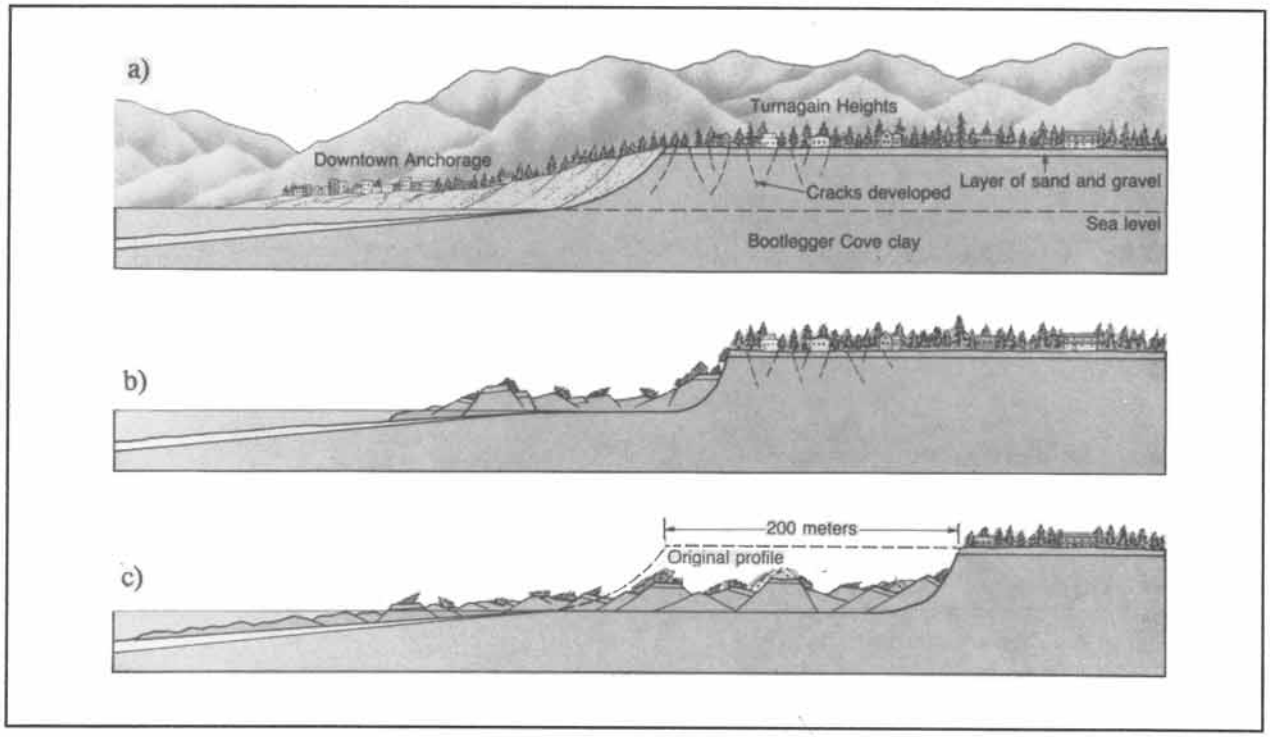

Figure 15-11: Collapse of the Turnagain Heights-district in Anchorage, Alaska, triggered by the 1964 earthquake. a) Opening of cracks, b) sliding, and c) final damage, five minutes after the onset of sliding.

Point Fermin, California. The major cause of sliding here is oversteepening of the cliffs. Obviously, the recurrence of multiple earthquakes in the region further contributes to the destabilization of the cliffs at Point Fermin.

Slides may, also, be triggered by an increase of the pore water pressure of rock formations, soaked by heavy rainfall or by the inadvertent effects of human construction work. The Vaiont Dam disaster, 1963, is a tragic example of construction with poor site investigation. The Vaiont Valley, Italy, was dammed by a 265-meter-tall hydropower dam, completed in 1960. The water reservoir, forming behind the dam, soaked the rocks of the walls of the Vaiont gorge. Creep of the walls, which included swelling clays and cavernous limestones, occurred at rates of one centimeter per week and speeded up to twenty centimeters per day in the weeks before the final collapse. Finally, Mount Toc's flank let loose 0.24 cubic kilometer of rock and debris, which filled the Vaiont Valley to 150 meters above the reservoir level (Fig. 15-13a). Consequently, the reservoir flooded the dam with a ninety-meter-high wall of water, leaving the Vaiont Dam miraculously intact, but destroying everything else in its path downstream; about 2,600 deaths were counted. The landslides of both the Vaiont disaster and the Gros Ventre slide (see, also, Fig. 1-7b) resulted from the swelling of a layer of clay beneath a surface slope, which was subparallel to the stratigraphic dip, termed a dip-slope. Figure 15-13b is a north-south cross-section of the Vaiont Valley and outlines the failure surface of the slide mass. The failure started by swelling and detachment of the clay-bearing Malm formation. The section of the Gros Ventre slide, Wyoming, suggests a similar mechanism of failure (Fig. 15-14). The slide occurred after a period of extensive rainfall, which destabilized the sandstone bed on a dip-slope of water-saturated clays.

Landslides seldom occur without precedents. Areas frequently affected by landslides commonly are littered with deposits of *allochtonous* rock sheets and jostled debris. Figure 15-15 illustrates the morphology of an old landslide in the landscape. Figure 15-16a shows a detailed geological map of the oversteepened northern slope of the

Figure 15-12: *Collapse of urbanized cliffs at Point Fermin, California.*

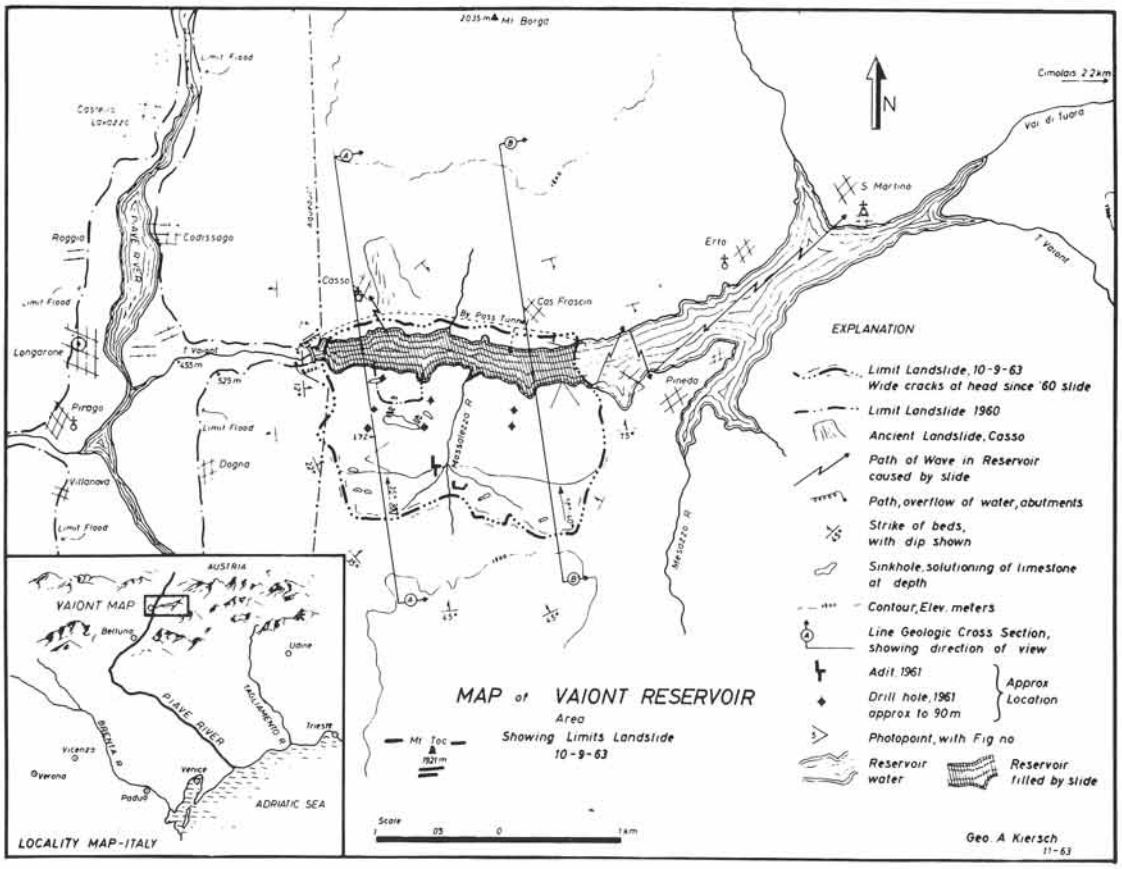

Figure 15-13a: *Geotechnical map of the Vaiont reservoir and the extent of the 1963 rockslide.*

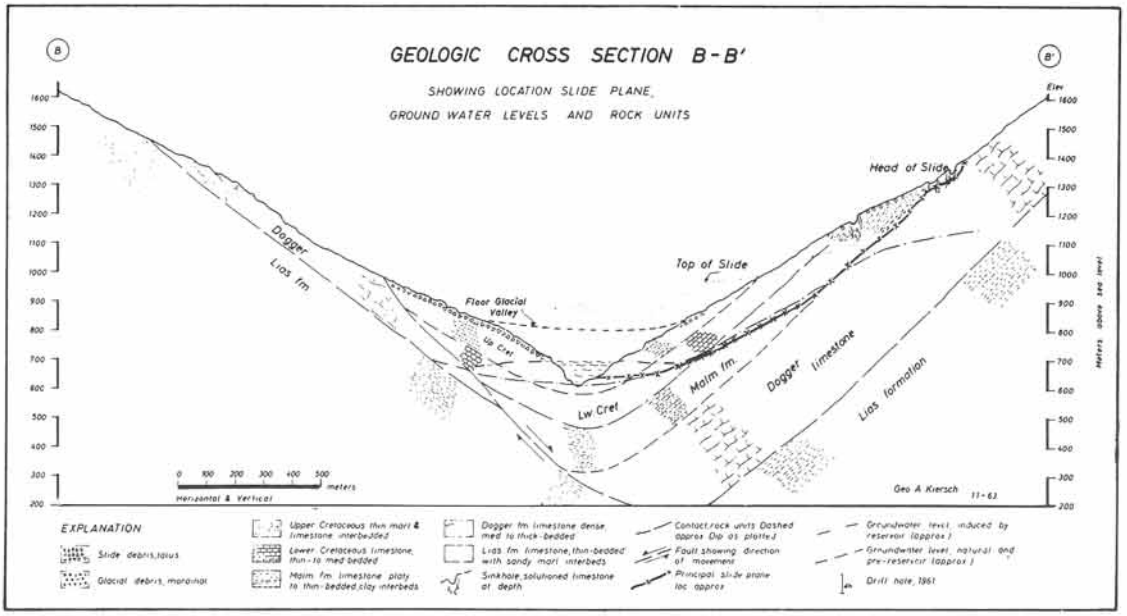

Figure 15-13b: *Unstable dip-slopes of stratigraphic bedding, overlying swelling clays, caused the Vaiont slide, Italy, 1963.*

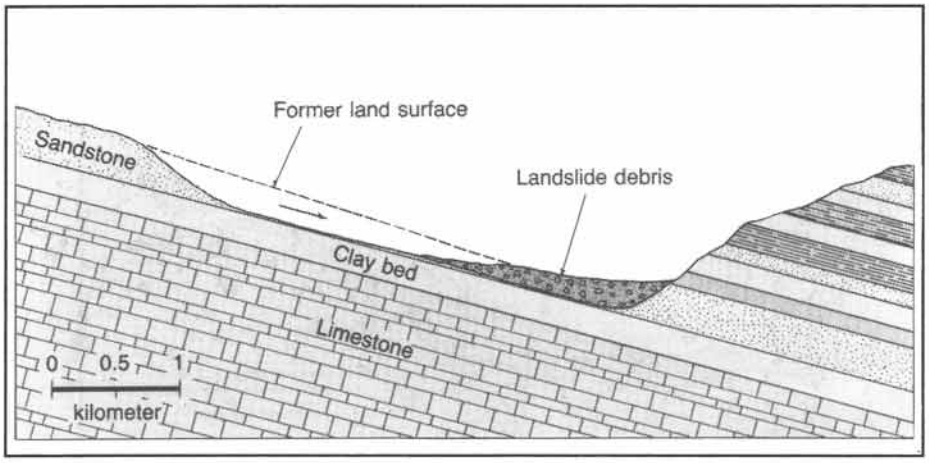

Figure 15-14: *Cross-section of the Gros Ventre slide, Wyoming, 1923.*

Sierra Alhamilla, Betic Cordillera, Spain. The village of Turrillas is built on top of, at least, four ancient rock slides (Fig. 15-14b). Turrillas is presently located below a potential landslide mass of three million tons of rock included in the unstable Cerro Minuto near the 1093-meter summit above the village. Incipient movement is indicated by open cracks at Cerro Minuto.

☐Exercise 15-2: The detailed drift map and cross-sections of the Turrillas area are shown in Figure 15-17a & b. a) Color the various slide masses, and estimate the surface area covered by ancient slides. b) Write a summary of the geological history.

Figure 15-15: *A classical example of an ancient (prehistoric) debris-flow, recognized as such from its geomorphology of altered volcanic rocks, Pahsimeroi River, South Idaho.*

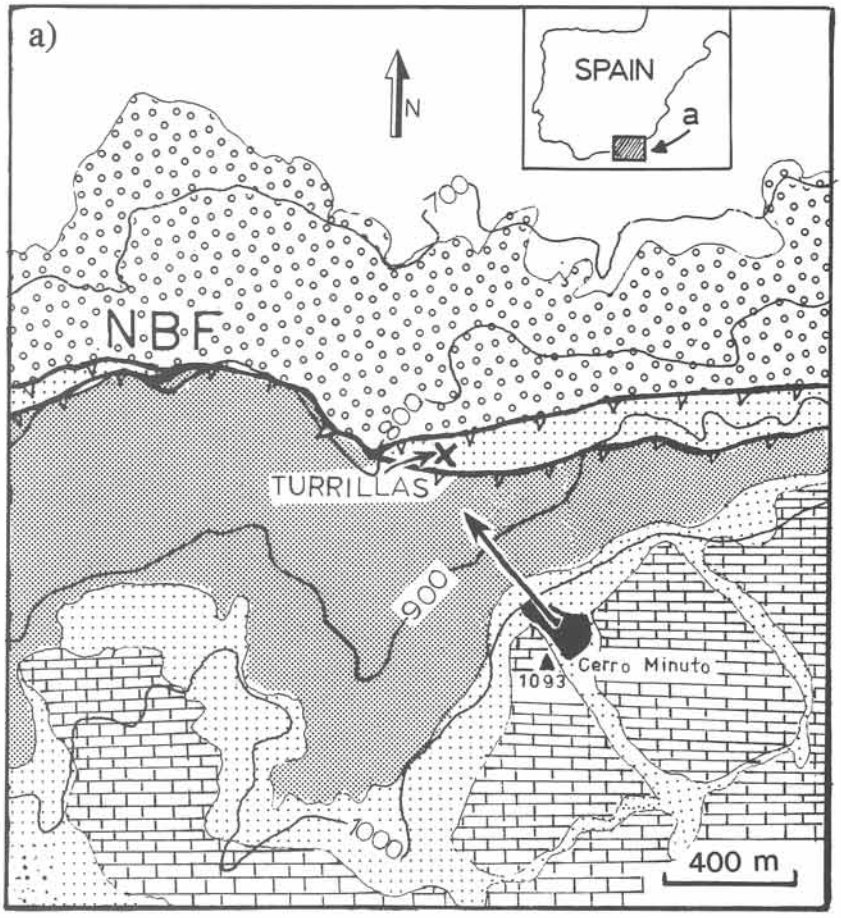

Figure 15-16: *Threat of rockslides near Turrillas, southeast Spain. a) Geological outcrop pattern of solid geology on topographic base map. The unstable limestone cliff of Cerro Minuto has a movement trajectory directed at Turrillas village. The Northern Boundary Fault (NBF) separates Tortonian clastics in the north wall from the uplifted metamorphic basement south of the fault. See Figure 15-17a for legend. b) View of Turrillas from Cerro Minuto. Locations 1 to 3 are sites of old rock slides, marked, also, on the drift map of Figure 15-17a.*

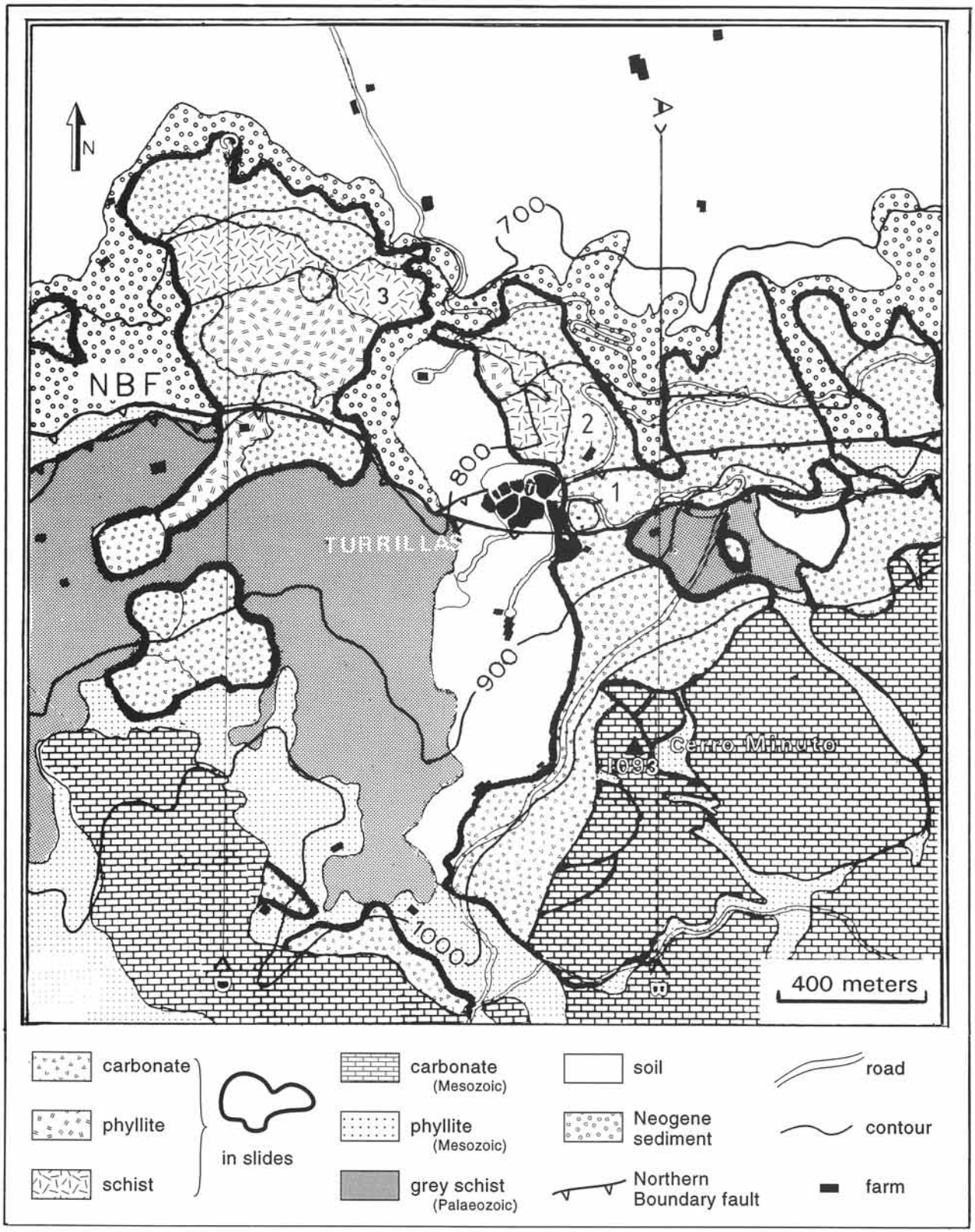

Figure 15-17a: *Drift map of the Turrillas area, showing extent of ancient slide masses. Compare with the map of solid geology for the same area in Figure 15-16a.*

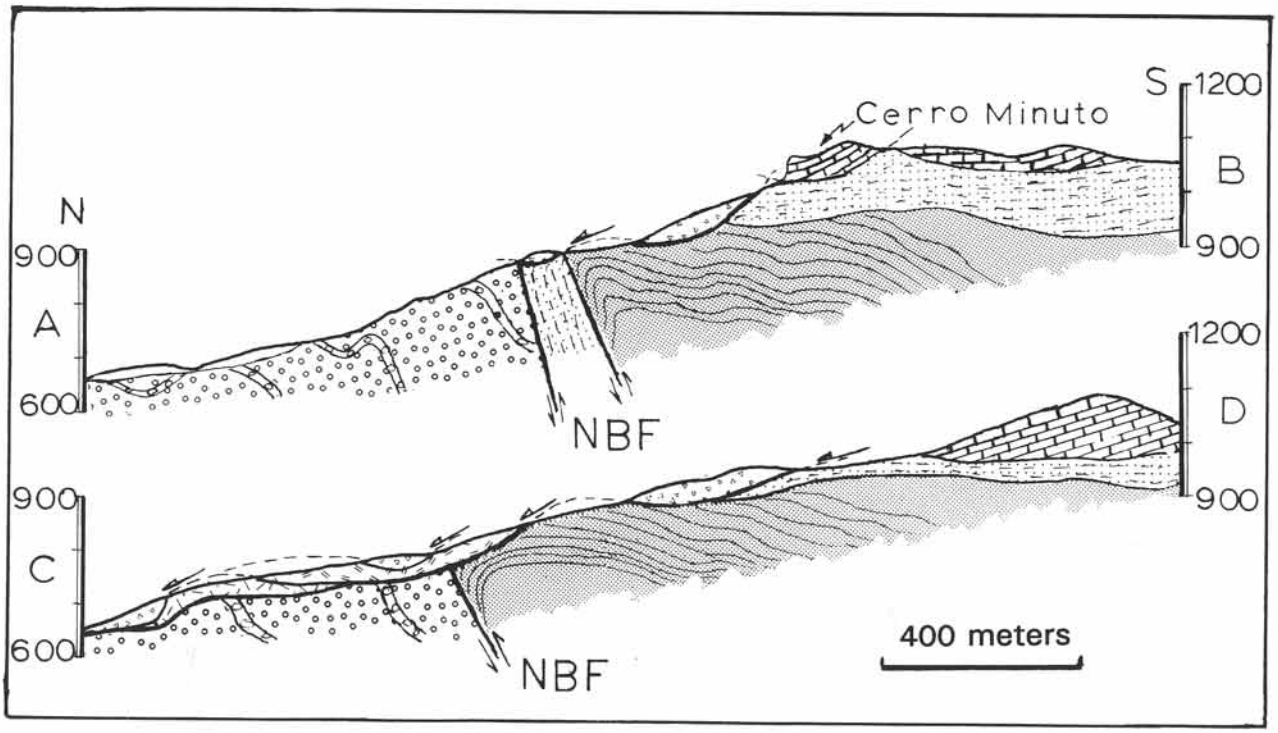

Figure 15-17b: *Cross-sections of the Turrillas slides along the locations outlined on Figure 15-17a.*

15-3 Sinkholes

Engineering projects may be severely delayed and overrun their budgets if large cavities and caves threaten to destabilize the support of huge construction. For example, the Keban Dam in eastern Anatolia, Turkey, was completed in 1974, three years after its scheduled opening and with enormous cost incurrence (Fig. 15-18). The dam is founded on karstic limestone, underlaid by impervious schist at 345 meters depth. The porous limestone section had to be cut off by a grout curtain and a buried concrete wall down to 345 meters to guarantee a reliable water cut-off. The main cause of the delay in this already ambitious operation was the discovery, during the construction work, of a huge solution cavity 330 meters below the crest of the dam. The cavity, measuring 138 meters long, 117 meters wide, and 30 meters high, was stopped with 60,000 cubic meters of concrete. The superstructure of the dam itself is only 170 meters high.

Solution cavities form in limestone by the solution and transport of calcium carbonate after seepage of corrosive ground water, that is slightly acidic if charged with organic carbon dioxide. The hydrologic circulation pattern may concentrate the corrosive ground water flow in particular fracture zones, but the pattern of solution caves and cavities is commonly chaotic (Fig. 15-19). The presence of solution cavities in the subsurface may sometimes be inferred from the occurrence of *sinkholes* at the surface. These are conspicuous collapse features, forming circular pits in the landscape, termed a *karst topography* if the sinkholes are abundant (Fig. 15-20a). A huge sinkhole in the Manati area, Puerto Rico, is utilized to support the Arecibo deep-space radio telescope (Fig. 15-20b). Pockmarked karst surfaces occur in the Mammoth Cave area, Kentucky; western Texas; Florida; and New Mexico, where the Carlsbad Caverns occur (Fig. 15-21).

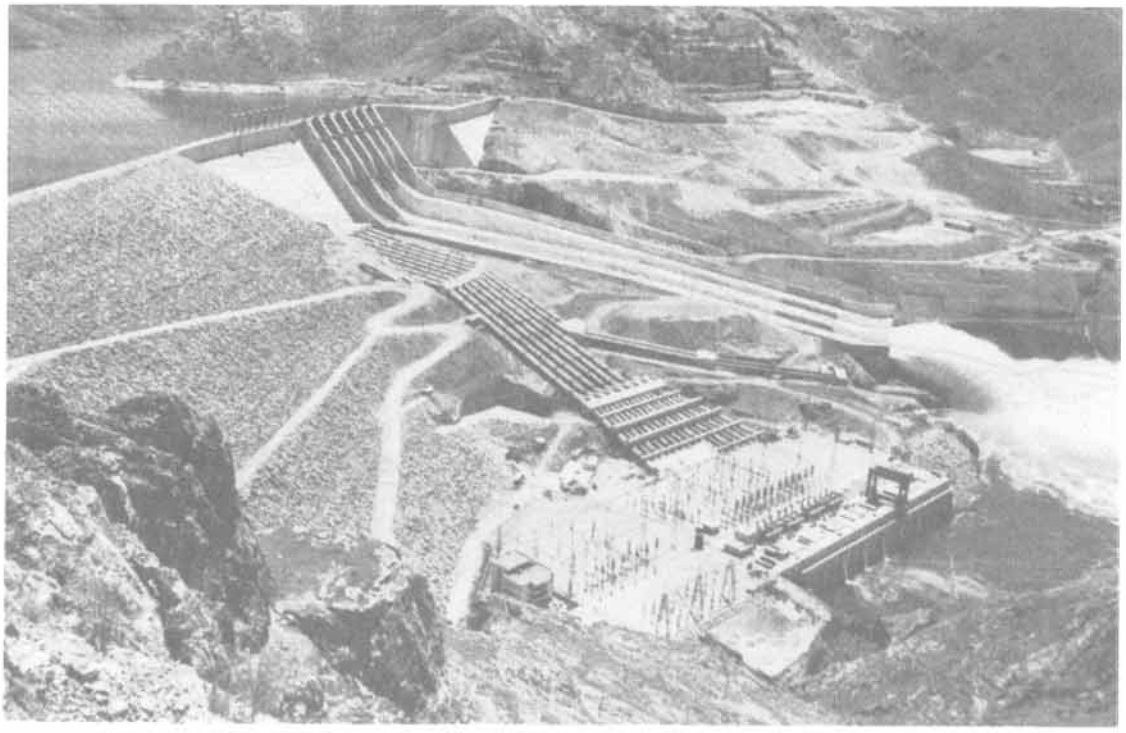

Figure 15-18: *Completed Keban hydropower dam, Turkey, which involved stabilization of the dam foundation by works down to 345 meters beneath the surface.*

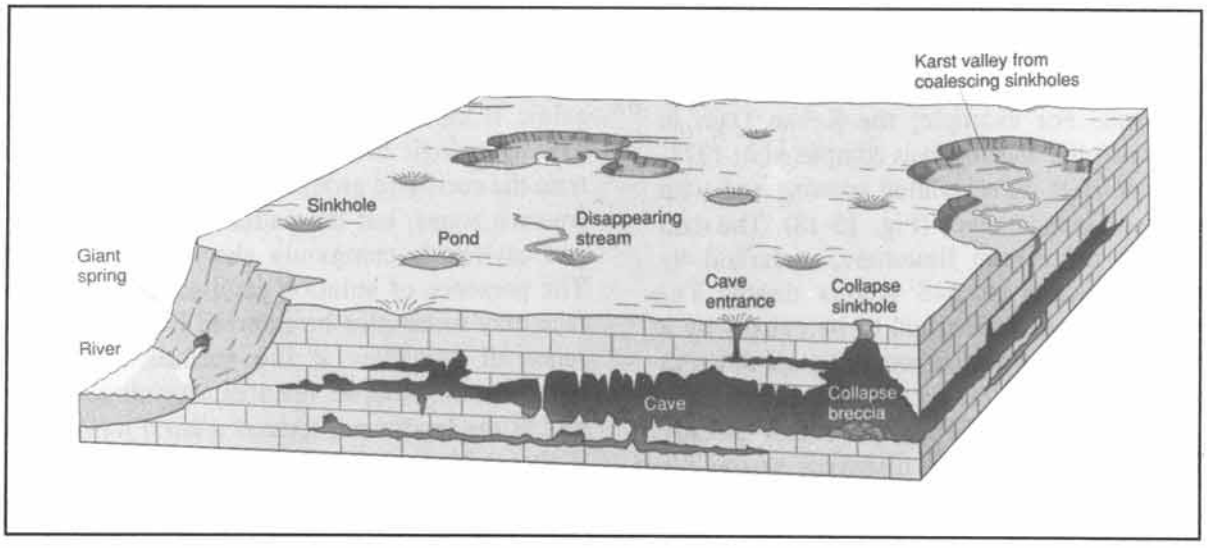

Figure 15-19: *Schematic block diagram of a karstic limestone formation with underground caves and surface sinkholes.*

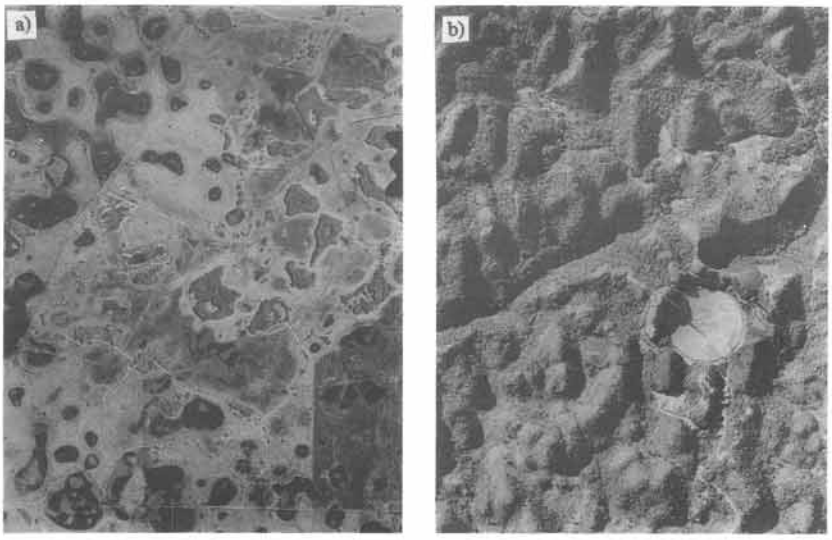

Figure 15-20: Two aerial views of karst landscapes: a) Florida, USA, b) Manati area, Puerto Rico.

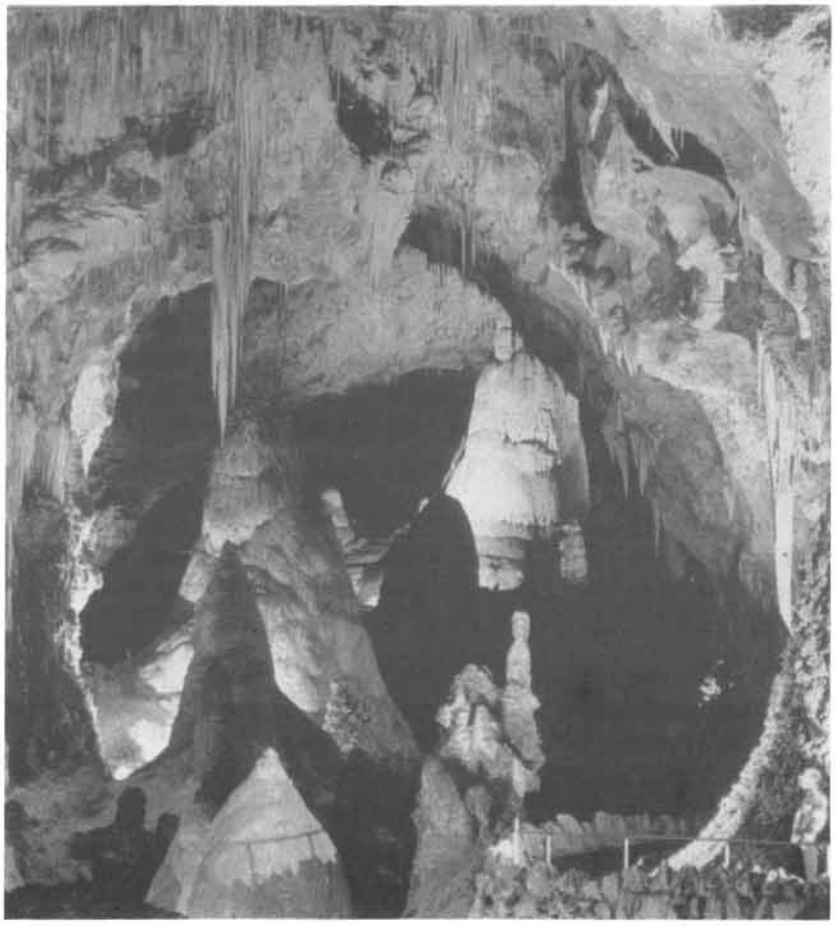

Figure 15-21: Underground solution cave at Carlsbad Caves, New Mexico.

☐Exercise 15-3:
a) What particular geological hazard threatens the urbanization of a karstic area?
b) Argue whether it is advisable to use sinkholes for uncontrolled waste disposal.

15-4 Glacial Structures

Huge portions of the continents have been covered by ice sheets during recurrent epochs of glaciation during past ice ages or *glacials*. The geological map pattern of many regions may be obscured by superficial deposits, laid down during past glacials. Ice is a crystalline substance and slowly spreads under its own weight like a drop of oil, but at extremely slow velocity. Nonetheless, any rubble and debris inside and on top of the ice sheets and glaciers is eventually transported to the rim of the ice expanse. Even when the ice masses retreat, we can recognize the former location of their margin because of the rock rubble or *moraines* accumulated in sinuous ridges across the landscape. Figure 15-22 illustrates such an end-moraine and the adjacent ground-moraine, left behind underneath the receding glacier. Beyond the area formerly covered by the glacier is the outwash plain, where glacial melt waters have deposited the mud-fraction or *till*. The outwash plain may feature pockmarks, termed *kettles*, that resemble sinkholes of karstic terrains.

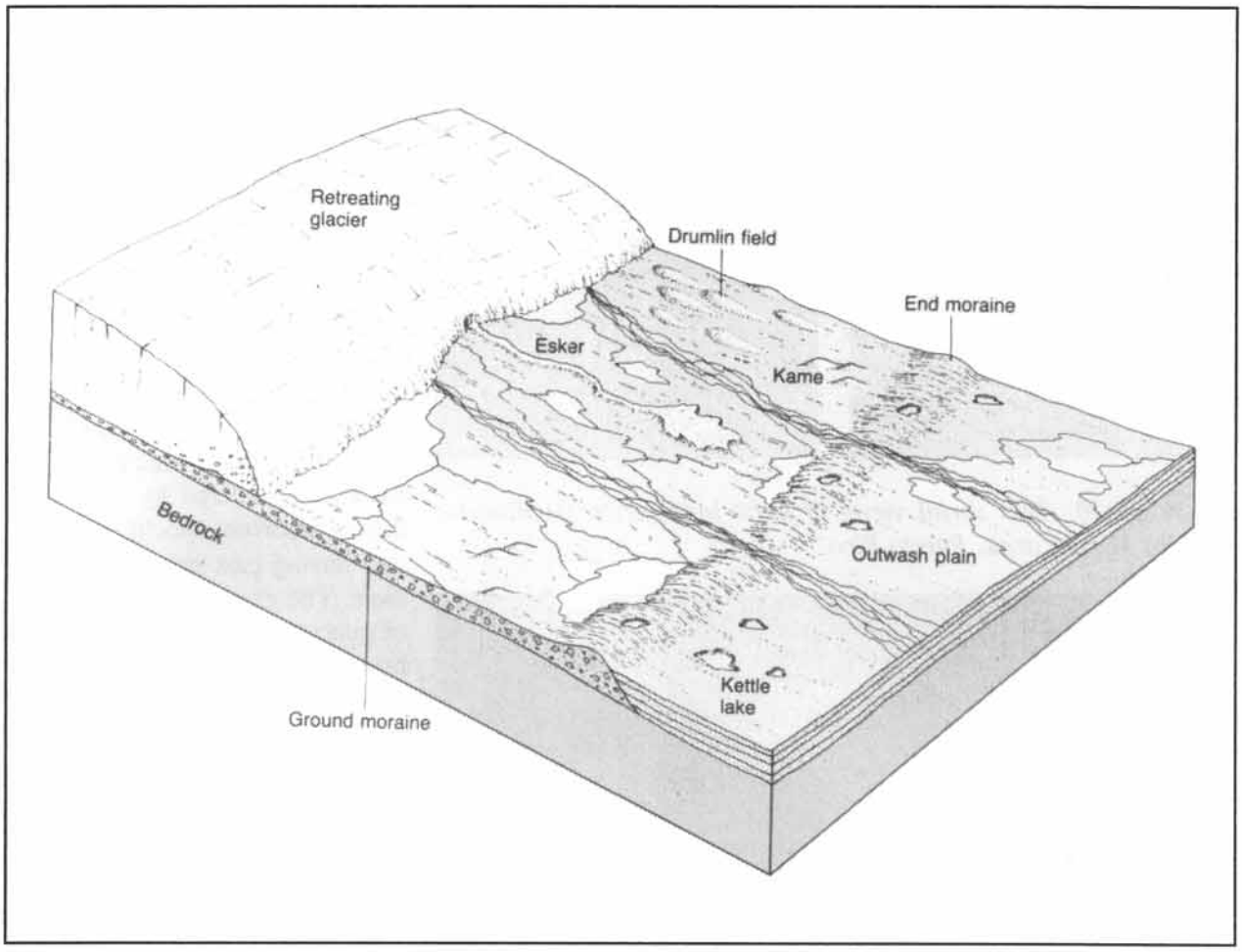

Figure 15-22: *Perspective diagram, showing the various superficial deposits left behind by a retreating glacier.*

However, kettles and kettle lakes are formed when blocks of ice stick into the till-mud and prevent the accumulation of any tills until they melt, thus leaving a pit or kettle in the outwash plain.

Other depositional patterns, found on the ground-moraine of glaciated terrains, are the eskers, drumlins, and kames. *Eskers* are narrow ridges of sedimentary rock that form in subglacial streams, while their lateral extent is constrained by the subglacial tunnel that holds the melt-water (Fig. 15-22). Once the glacier retreats, the esker deposits form topographic ridges in the terrain. *Drumlins* range in height from fifteen to fifty meters and occur in groups of parallel, elongated, small hillocks, resembling a group of whales, surfacing in the ocean (Fig. 15-22). It is assumed that drumlins are molded from the unconsolidated deposits beneath an advancing glacier. *Kame* terraces are steep-sided hills, deposited by melt-water in openings within the glacier. They form isolated and irregular mounds.

☐Exercise 15-4: Figure 15-23 illustrates the end-moraines in the Great Lakes region, North America, deposited during the Wisconsinian glacial, that lasted from 150,000 to 10,000 years ago. Distinguish and interconnect the various moraines that mark the different, temporal maximum expansions of the ice front. Were the Wisconsinian end-moraines formed before or after the Illinoisian end-moraines?

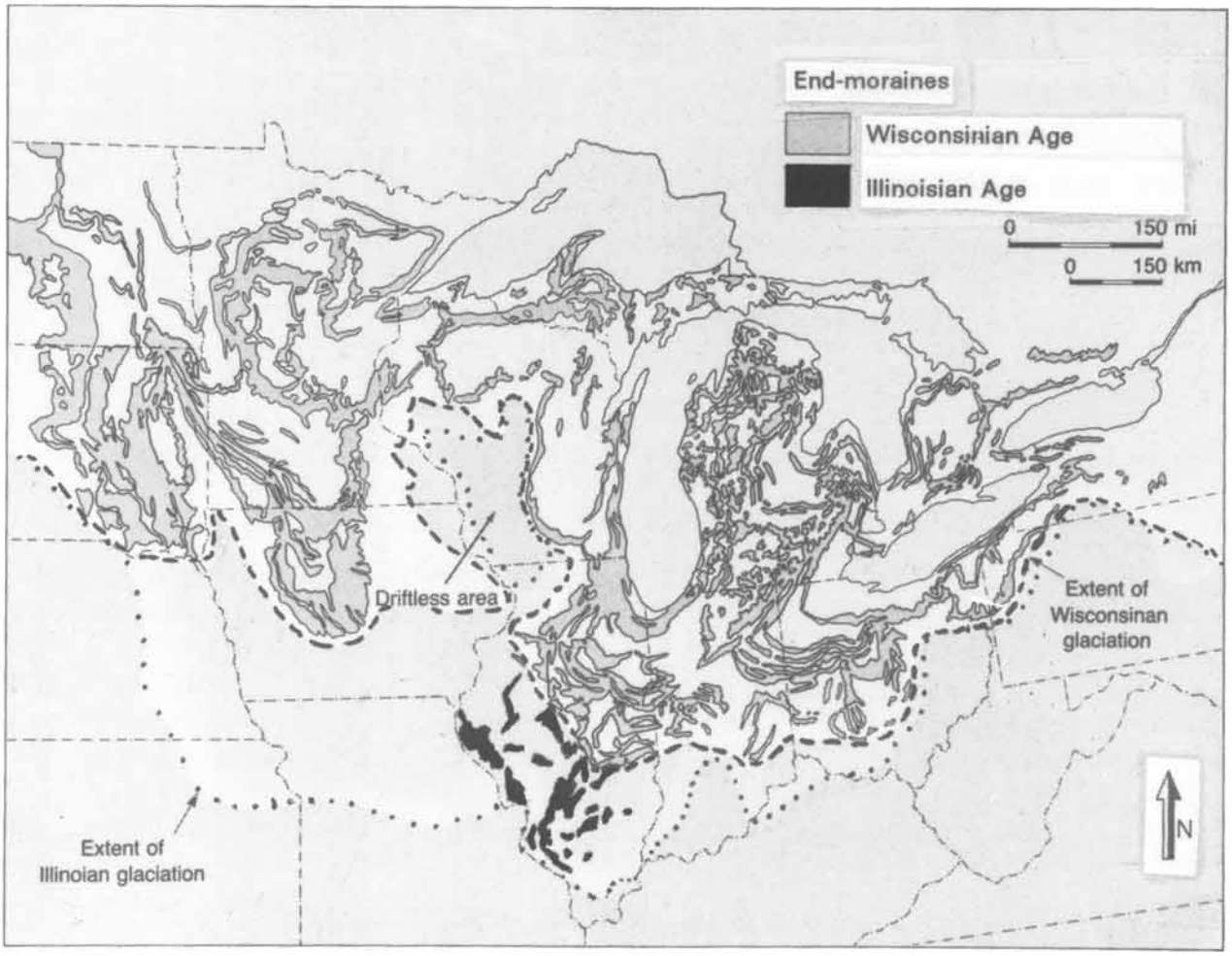

Figure 15-23: Wisconsinian and Illinoisian end-moraines in the Great Lakes region, North America.